Robust Doppler Spread Estimation in the Presence of a Residual Carrier Frequency Offset

Mehrez Souden, Sofiène Affes, Jacob Benesty, and Rim Bahroun

***Abstract*—In high data-rate transmission systems, accurate Doppler spread estimation is a critical task for not only mobile velocity estimation, but also for optimal adaptive processing. It is known that the residual carrier frequency offset (CFO) which is inherent to the asynchrony between the communicating ends in a wireless link has a detrimental effect on the Doppler spread estimation. In this correspondence, we propose a new simple and accurate approach that copes with this issue by explicitly taking the CFO into account when estimating the Doppler spread. This new approach stems from the fact that the cross-correlation of the channel is a weighted summation of monochromatic plane waves (or an inverse Fourier transform of its power spectral density). It turns out that these plane waves are locally (as compared to the sampling rate) distributed around a main frequency which is nothing but the CFO. Using this property, we base our analysis on Taylor series expansions in addition to an observation temporal aperture to develop a two-ray spectrum approximate model for the Doppler spread estimation. We find that the Doppler spread is half of the frequency spacing between both rays which are located symmetrically around the CFO. Finally, we deduce new closed-form estimators for the Doppler spread and also for the CFO. These estimators are accurate and practical in environments with isotropic scattering where the channel power spectrum density (PSD) is symmetric. Simulations are provided to illustrate the advantages of the proposed method and its robustness to the CFO.**

***Index Terms*—Carrier frequency offset, Doppler spread, Doppler spread factor, maximum Doppler frequency, two-ray spectrum approximation.**

I. Introduction

The Doppler spread is inherent to wireless communication systems since it is caused by the motion of one of the communicating ends with respect to the other [1]. Its estimation is extremely important in these systems. Indeed, with the knowledge of this parameter, the velocity of the mobile terminal can be exactly recovered [6], [7] and the optimal adaptation step-size can be properly tuned for optimal adaptive processing in wireless communications [13]. Another common aspect in wireless systems is the carrier frequency offset (CFO) which is caused by the physical limitation of the oscillators at the receiver and the emitter to properly identify the carrier frequency and down- (or up-) convert the signals of interest. Unfortunately, it turns out that the CFO has a detrimental effect on the existing Doppler spread estimation techniques as supported by simulations in Section V (further details are provided therein). This fact accounts for the need to develop an efficient method for Doppler spread estimation which is robust to the CFO.

Herein, we make a clear distinction between the *maximum Doppler frequency* and the *Doppler spread factor*. While it is understood that the first is the maximum frequency shift caused by the Doppler phenomenon, the second stands for the standard deviation of the frequency around the CFO. Despite the direct relationship between both parameters [see (14) below], the deduction of one of them knowing the other requires the knowledge of the shape of the channel's PSD. The proposed technique is able to determine the Doppler spread factor using the unique symmetry assumption on the channel's PSD. This assumption is valid in wireless environments with isotropic scattering, i.e., where the signal transmitted by the mobile terminal reaches the base station from all angles equiprobably [1], [6], [7].

So far, several techniques have been proposed to characterize the Doppler effect due to its importance in the design of adaptive communication systems. For instance, Hansen *et al.* proposed a maximum likelihood (ML)-based approach in [2] where the channel is assumed to follow the Jakes' model [1]. The maximization of the similarity between the PSD of the detected channel and a hypothetical one (corresponding to the Jakes' model) leads to good estimates of the maximum Doppler frequency. Level crossing rate (LCR)-based techniques have been proposed in [3], [4]. These techniques take advantage of the direct relationship between the fading rate and the maximum Doppler frequency. Other approaches which are based on the channel covariance at different time lags have been also proposed in [5]–[7], for example. The latter techniques are known to be generally more efficient than LCR-based ones [5], [6]. To the best of our knowledge, most of these techniques were developed under the assumption of no CFO. This assumption is not practical since the CFO is inherent to the physical limitations of the oscillators at the receiver and the transmitter in wireless links. As an example, third generation partnership project (3 GPP) standards tolerate a CFO of up to 200 Hz at 2-GHz carrier frequency after RF down-/up-conversion (i.e., 0.1 ppm at the base station) [8]. It turns out that the performance of these wireless transceivers depends on the CFO in addition to the conventional parameters [e.g., signal-to-noise ratio (SNR), and observation window length].

In this correspondence, we propose a new simple and accurate approach to estimate the Doppler spread factor which is robust to the CFO. This new approach stems from the fact that the cross-correlation of the channel is the inverse Fourier transform of its PSD. In other words, this cross-correlation can be seen as a weighted summation of monochromatic plane waves. In the case of the Doppler spread, these plane waves are locally distributed around the CFO, as compared to the sampling rate. Indeed, the channel spectrum has small fluctuations which are local and focused around the CFO. We take advantage of this feature jointly with a temporal aperture to develop a new two-ray approximate model that allows us to find a simple and accurate closed-form estimator of the Doppler spread factor without the knowledge of the shape of the channel's PSD.[1] As a byproduct of this contribution, we also develop a CFO estimator and show its robustness through numerical evaluations.

This correspondence is organized as follows. Section II describes the data model. Section III reviews some important properties of the channel that will be used in the remaining part of this correspondence and the approximate form of the channel correlation matrix that can be found by taking into account the local deviations of the channel spectrum around the CFO. Section IV outlines the proposed new closed-form Doppler spread estimator in the presence of CFO. Section V evaluates the performance of the proposed method through some numerical examples. Finally, we draw out some conclusions in Section VI.

[1]Robustness to the Doppler type and classification of the Doppler spread with respect to its spectrum shape in order to systematically retrieve the maximum Doppler frequency from the spread factor is still under investigation.

Manuscript received October 08, 2008; accepted April 08, 2009. First published May 15, 2009; current version published September 16, 2009. The associate editor coordinating the review of this manuscript and approving it for publication was Dr. Shengli Zhou. This work was supported in part by a Canada Research Chair in Wireless Communications. This work was published in part in the *Proceedings of the Ninth IEEE International Workshop on Signal Processing Advances in Wireless Communications* (SPAWC), Recife, Brazil, July 6–9, 2008, pp. 31–35.

The authors are with the Université du Québec, INRS-EMT, Montréal, QC H5A 1K6, Canada (e-mail: souden@emt.inrs.ca).

Color versions of one or more of the figures in this paper are available online at http://ieeexplore.ieee.org.

Digital Object Identifier 10.1109/TSP.2009.2022859

II. Data Model

Let $s(t)$ denote a source signal propagating through a channel $h(t)$ and impinging on a receiving antenna at instant t. An additive noise $v(t)$ is generally present and the resulting signal observed by the receiving end is expressed as [1]–[7]:

$$x(t) = h(t)s(t) + v(t). \tag{1}$$

This situation is typical in wireless communication systems where $s(t)$ models a signal transmitted by a mobile terminal and $x(t)$ is the signal observed at the base station. Here, we assume that $s(t)$ is a training data. Without loss of generality, we further assume that $s(t) = 1$, in which case $x(t)$ can be seen as an estimate of the channel $h(t)$ and $v(t)$ as a residual estimation error. Moreover, we assume that the channel, $h(t)$, is a wide sense stationary (WSS) process and that the noise, $v(t)$, is zero-mean with temporally independent and identically distributed (i.i.d.) components [5].

Again, our aim in this work is to accurately estimate the Doppler spread factor (and deduce the maximum Doppler frequency when the PSD shape is available) even in the presence of the CFO. The former parameter is denoted as σ_f (f_d stands for the maximum Doppler frequency) while the CFO is denoted as f_c. The proposed approach is based on the analysis of the observed signal over a given observation window of length N (taking N time snapshots $nT_s, (n+1)T_\mathrm{s} \cdots, (n+N-1)T_\mathrm{s}$, where T_s is the sampling rate, n and N are positive integers). Under the above assumptions, the observations' covariance matrix is then expressed as

$$\mathbf{R}_x = E\{\mathbf{x}(nT_s)\mathbf{x}^H(nT_s)\} = \mathbf{R}_h + \mathbf{R}_v \tag{2}$$

where

$$\mathbf{x}(nT_s) = [x[nT_s] \cdots x[(n+N-1)T_\mathrm{s}]]^T \tag{3}$$

$$\mathbf{R}_h = E\{\mathbf{h}(nT_s)\mathbf{h}^H(nT_s)\} \tag{4}$$

$$\mathbf{h}(t) = [h[nT_s] \cdots h[(n+N-1)T_\mathrm{s}]]^T \tag{5}$$

$$\mathbf{R}_v = E\{\mathbf{v}(nT_s)\mathbf{v}^H(nT_s)\} = \sigma_v^2\mathbf{I}_N \tag{6}$$

$$\mathbf{v}(t) = [v[nT_s] \cdots v[(n+N-1)T_\mathrm{s}]]^T \tag{7}$$

where σ_v^2 is the noise variance, $\mathbf{I}_N$ is the identity matrix of size $N \times N$, $(\cdot)^T$ is the transpose of a vector or a matrix, and $(\cdot)^H$ is the transconjugate operator.

III. Key Properties of the Channel Covariance Matrix

In what follows, we will use the following notations: $\omega = 2\pi f, \omega_\mathrm{d} = 2\pi f_\mathrm{d}, \sigma_\omega = 2\pi\sigma_f, \omega_\mathrm{c} = 2\pi f_\mathrm{c}$, and $\tau_{lk} = (l-k)T_\mathrm{s}$ with $l,\ k \in \{0, \cdots, N-1\}$. f and ω are related up to a 2π scaling factor and so are σ_ω and σ_f. Hence, estimating f_c is equivalent to estimating ω_c (so is the case for σ_ω and σ_f). Now, by assuming that the channel is WSS, we express its cross-correlation taken at two instants $t_l = lT_s$ and $t_k = kT_s$ using its PSD $S(\omega)$ as:

$$r_h(\tau_{lk}) = \frac{\sigma_h^2}{2\pi}\int_{\omega_\mathrm{c}-\omega_\mathrm{d}}^{\omega_\mathrm{c}+\omega_\mathrm{d}} S(\omega)e^{j\omega\tau_{lk}}d\omega \tag{8}$$

$$= \sigma_h^2 e^{j\omega_\mathrm{c}\tau_{lk}}\int_{-\omega_\mathrm{d}}^{\omega_\mathrm{d}} \tilde{S}(\omega)e^{j\omega\tau_{lk}}d\omega \tag{9}$$

where σ_h^2 is the channel variance. In (8), we see that the channel cross-correlation at a given time lag τ_{lk} is a weighted summation of several monochromatic waves (or rays) which are distributed around the main ray at $\omega = \omega_\mathrm{c}$. In the case of the Doppler spread, these frequency deviations are small as compared to the sampling rate, thereby accounting for the Taylor series expansions that we will use in the sequel. In (9), $\tilde{S}(\omega) = (1/2\pi)S(\omega+\omega_\mathrm{c})$ and is in many practical cases symmetric [1], [9]. To sum up, we make the following two important assumptions.

- *Assumption 1*: The channel's PSD is symmetric. This assumption helps us to get rid of the second and third order frequency moments[2] when devising the two-ray spectrum approximation (see below and the proof in the Appendix). It is commonly made in the literature to model an isotropic scattering around the source signal [1], [6], [7], [9]. Anisotropic scattering breaks this assumption. This case falls beyond the scope of this work and we refer the readers to [6], for instance, for further details about this issue.
- *Assumption 2*: The frequency deviations are small as compared to the sampling rate. This assumption is also fundamental in our method since it allows us to use the second-order Taylor series to expand $\mathbf{a}(\omega+\omega_\mathrm{c})$ [see (11) below] and fourth-order expansions to approximate $\mathbf{R}_h$. It is valid in common wireless systems where the mobile terminals have relatively low to moderate speed and/or high data rates.

Based on Assumption 1, we deduce that the integral quantity in (9) is real. Consequently, the phase of $r_h(\tau_{lk})$ bears the information about ω_c while its magnitude is a function of σ_ω (or ω_d). In the sequel, we take advantage of both terms to properly estimate the Doppler spread factor. The overall channel covariance matrix defined in (4) is given by:

$$\mathbf{R}_h = \sigma_h^2\int_{-\omega_\mathrm{d}}^{\omega_\mathrm{d}} \tilde{S}(\omega)\mathbf{a}(\omega+\omega_\mathrm{c})\mathbf{a}^H(\omega+\omega_\mathrm{c})d\omega \tag{10}$$

where

$$\mathbf{a}(\omega) = [1\ e^{j\omega T_\mathrm{s}} \cdots e^{j(N-1)\omega T_\mathrm{s}}]^T \tag{11}$$

and the (l,k)th entry of $\mathbf{R}_h$ is defined as $[\mathbf{R}_h]_{lk} = r_h(\tau_{lk})$.

The core idea of the proposed approach is based on Assumption 1 and Assumption 2. Indeed, the problem of estimating f_d using (10) and (11) appears to be very similar to addressing the issue of angular spread (AS) and nominal angle-of-arrival (AOA) estimation for locally and incoherently scattered sources using an array of sensors. Referring to [10] and [11], for instance, we see that the same form (10)–(11) of the covariance matrix is also involved in the calculation of the AS and the nominal AOA but with a spatial frequency (function of the ray direction-of-arrival) instead of the temporal frequency, used in the current context. The estimation of the CFO and the Doppler spread seems, then, analogous to the estimation of the nominal AOA and AS, respectively. The latter issue has been addressed in several ways over the last few years. A notable solution was proposed in [11] and enhanced in [10] where the spatially spread source is approximated by two virtual point sources which are spatially separated by twice the AS value. Following this analogy and the detailed proof in the Appendix, we expect the second-order Taylor series expansions of $\mathbf{a}(\omega)$ in (10) around ω_c [fourth-order Taylor series expansions of the matrix $\mathbf{a}(\omega)\mathbf{a}^H(\omega)$] to provide an accurate and simple estimate of σ_ω. Indeed, we can express $\mathbf{R}_h$ as (see the Appendix for full details):

$$\mathbf{R}_h \approx \frac{\sigma_h^2}{2}\mathbf{A}(\omega_\mathrm{c}-\sigma_\omega, \omega_\mathrm{c}+\sigma_\omega)\mathbf{A}^H(\omega_\mathrm{c}-\sigma_\omega, \omega_\mathrm{c}+\sigma_\omega), \tag{12}$$

with

$$\mathbf{A}(\omega_\mathrm{c}-\sigma_\omega, \omega_\mathrm{c}+\sigma_\omega) = [\mathbf{a}(\omega_\mathrm{c}-\sigma_\omega)\mathbf{a}(\omega_\mathrm{c}+\sigma_\omega)]. \tag{13}$$

In Fig. 1, we show the theoretical variations of the channel's PSD and the locations of both frequency rays at $\omega_\mathrm{c} \pm \sigma_\omega$ in the approximate form

[2]The kth frequency moment is defined as $\mathcal{M}_k = \int_{-\omega_d}^{\omega_d} \omega^k \bar{S}(\omega)d\omega$.

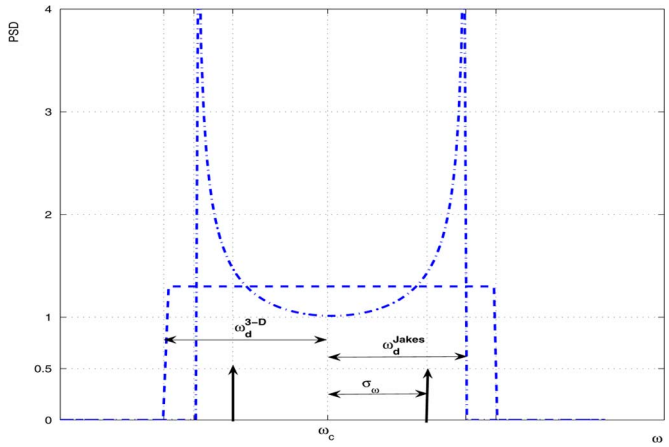

Fig. 1. Normalized theoretical channel's PSD variations (dashed lines) and locations of the approximate two rays (at $\omega_c - \sigma_\omega$ and $\omega_c + \sigma_\omega$) in the particular cases of Jakes (U-shaped PSD) and 3-D (flat PSD) channel models.

in (12) and (13) in both cases of Jakes and three-dimensional (3-D) scattering models [1], [9]. Clearly, estimating σ_ω amounts to localizing two rays separated by $2\sigma_\omega$ and symmetrically located around the CFO. We further provide the following two important remarks.

Remark 1: The estimation of the Doppler spread factor is independent of the Doppler distribution. However, if we are interested in estimating $f_{\rm d}$ (e.g., to determine the velocity of the mobile terminal), we need a prior knowledge of the distribution shape. In this case, we can use the straightforward relationship

$$\sigma_\omega = \left(\int_{-\omega_{\rm d}}^{\omega_{\rm d}} \omega^2 \tilde{S}(\omega) d\omega \right)^{1/2} \tag{14}$$

leading to

$$\omega_{\rm d} = \begin{cases} \sqrt{2}\,\sigma_\omega & \text{for Jakes' model} \\ \sqrt{3}\,\sigma_\omega & \text{for 3-D scattering model.} \end{cases} \tag{15}$$

Remark 2: As a built-in feature inherent to the proposed Doppler spread estimator, we are also able to estimate the CFO regardless of the frequency distribution (i.e., the PSD) provided that the latter is only symmetric around a central ray (f_c). The accuracy of this CFO estimator will also be highlighted in Section V.

In order to develop our Doppler spread estimator in the next section, we need to mention an important property of the channel covariance matrix model in (12) and (13). Indeed, in the particular case of no frequency spread (i.e., $\sigma_\omega = 0$), the matrix $\mathbf{R}_h$ reduces to $\mathbf{R}_h = \mathbf{a}(\omega_{\rm c})\mathbf{a}^H(\omega_{\rm c})$ which is of rank one. Thus, one can use a point source localization algorithm to estimate the CFO (see [10] and references therein). In the presence of the Doppler spread, we deduce from (12) and (13) that $\mathbf{R}_h$ is approximately of rank two (in essence due to the small channel frequency fluctuations around $f_{\rm c}$, as compared to the sampling rate). Consequently, we use this property to estimate the noise variance. In practice, we only have an estimate of $\mathbf{R}_x$ (denoted $\hat{\mathbf{R}}_x$). Knowing that $\mathbf{R}_h$ is almost rank deficient and assuming that the noise is temporally i.i.d., we are able to estimate the noise variance, σ_v^2, by averaging over the last smallest eigenvalues of $\hat{\mathbf{R}}_x$, and subsequently exploit it in the Doppler spread estimator proposed below.

IV. Doppler Spread Estimation With Carrier Frequency Offset

The two-ray spectrum approximation in (12) and (13) can now be efficiently used to determine σ_f and $f_{\rm c}$. We adapt the estimators that we proposed in our previous work [10] in the context of nominal AOA and AS estimation to the current problem. Indeed, according to (12)–(13), the (l,k)th entry of $\mathbf{R}_h$ can be expressed as

$$r_h(\tau_{lk}) \approx \sigma_h^2 \cos(2\pi\tau_{lk}\sigma_f) e^{j2\pi f_{\rm c}\tau_{lk}}. \tag{16}$$

Taking into account (2) and (16), the expression for the (l,k)th entry of $\mathbf{R}_x$ is

$$r_x(\tau_{lk}) \approx \sigma_h^2 \cos(2\pi\tau_{lk}\sigma_f) e^{j2\pi f_{\rm c}\tau_{lk}} + \sigma_v^2 \delta(\tau_{lk}) \tag{17}$$

where $\delta(\tau_{lk})$ is the Dirac function. It is easy to see from (17) that the entries of the mth ($m = k-l \in \{-(N-1), \ldots, N-1\}$) sub-diagonal of the matrix $\mathbf{R}_x$ are all identical (i.e., $\mathbf{R}_x$ is Toeplitz). To simplify the notations and in contrast to [15], we will consider the index m instead of the double indexing (k,l). In other words, we will be using τ_m instead of τ_{lk} in the sequel.[3] In practice, $\mathbf{R}_x$ is unavailable, but can be estimated using T data samples

$$\hat{\mathbf{R}}_x = \frac{1}{T} \sum_{n=1}^{T} \mathbf{x}(nT_s)\mathbf{x}^H(nT_s) = \hat{\mathbf{R}}_h + \hat{\sigma}_v^2 \mathbf{I}_N. \tag{18}$$

Each entry of the mth subdiagonal of this matrix, $\hat{r}_x(\tau_m)$, is a consistent estimate of $r_x(\tau_m)$. In particular, when $\tau_m = 0$ (i.e., $m = 0$), we obtain $r_x(0) = \sigma_h^2 + \sigma_v^2$ whose estimate is $\hat{r}_x(0) = \hat{\sigma}_h^2 + \hat{\sigma}_v^2$. As we stated previously, we average over the last smallest eigenvalues of $\hat{\mathbf{R}}_x$ to calculate $\hat{\sigma}_v^2$. Then, we deduce $\hat{\sigma}_h^2$ as

$$\hat{\sigma}_h^2 = \hat{r}_x(0) - \hat{\sigma}_v^2. \tag{19}$$

To calculate the estimators of σ_f and $f_{\rm c}$ ($\hat{\sigma}_f$ and $\hat{f}_{\rm c}$, respectively), we use $\hat{r}_x(\tau_m)$ for $m > 0$ and minimize the following cost function:

$$J^{(m)}(f_{\rm c}, \sigma_f) = \left| \hat{r}_x(\tau_m)/\hat{\sigma}_h^2 - \cos(2\pi\tau_m\sigma_f) e^{j2\pi f_{\rm c}\tau_m} \right|^2 \tag{20}$$

with respect to $f_{\rm c}$ and σ_f. Straightforward calculations lead to the following estimators[4] [10]:

$$\hat{f}_{\rm c}^{(m)} = \frac{1}{2\pi\tau_m} \angle\{\hat{r}_x(\tau_m)\} \tag{21}$$

$$\hat{\sigma}_f^{(m)} = \frac{\arccos\left(\Re\left\{ \hat{r}_x(\tau_m) e^{-j2\tau_m\pi\hat{f}_{\rm c}}/\hat{\sigma}_h^2 \right\} \right)}{2\pi\tau_m} \tag{22}$$

where $\angle\{\cdot\}$ is the angle operator and $\Re\{\cdot\}$ is the real part of the complex number between brackets. A similar form of only the CFO estimator has been proposed in [14]. However, no clarification was provided therein on the choice of the appropriate time lags that have to be used to obtain an accurate estimate of CFO. Referring to [10] and [11], we find that the estimation of f_c and σ_f is analogous to the estimation of the nominal AOA and the AS of a locally scattered source, respectively. We take advantage of this analogy to deduce an efficient way to choose the optimal time delays when using (21) and (22). In fact, we infer from the asymptotic performance analysis in [10] (specifically, Theorem 1 therein) that the smallest positive values of τ_m lead to accurate estimates of f_c, while large values [near the first sign change of $\Re\{\hat{r}_x(\tau_m)e^{-j2\tau_m\pi\hat{f}_{\rm c}}\}$ for the Jakes and 3-D scattering models considered herein, for example] lead to accurate estimates of σ_f. Taking inappropriate values of the time delay in (21) and (22) may degrade the performance of the estimators as shown in [10]. Now, based on the knowledge of the channel's PSD shape and σ_f (or σ_ω), we can deduce $f_{\rm d}$ (or $\omega_{\rm d}$) using (14) [particularly (15) in the case of Jakes and 3-D scattering models]. Finally, we also see from (21) that even though our focus was on the estimation of the Doppler spread, we developed a new

[3] In practice, we simply estimate the channel correlation at different time lags and form the estimate of the matrix $\mathbf{R}_x$ using the fact that the channel is WSS.

[4] In the ideal case of no CFO, we force $\hat{f}_c = 0$ in (22).

estimator of the CFO that will be shown to be very accurate by simulations.

To implement (21) and (22), instead of using a single time delay to estimate f_c and σ_f, we use $p > 1$ time lags and obtain p estimates for each parameter. Then, reliable estimates are obtained by a simple averaging as

$$\hat{f}_c = \frac{1}{p}\sum_{m=1}^{p} \hat{f}_c^{(m)}, \tag{23}$$

$$\hat{\sigma}_f = \frac{1}{p}\sum_{m=1}^{p} \hat{\sigma}_f^{(m)}. \tag{24}$$

The choice of the parameter p in (23) and (24) is rather empirical. Indeed, due to the small values of the lag step T_s, one can empirically verify that neighboring values of the time lag lead to very similar performance when estimating either the CFO or the Doppler spread. In our case, we found after extensive simulations that $p = 20$ leads to good performance while keeping low complexity in all the scenarios investigated in Section V. In practice, we need to calculate the received signal covariances at $2p + 1 \leq N$ positive time lags only (i.e., the $p + 1$ smallest and p largest possible time lags). We use the first time lag $\tau_0 = 0$ to estimate $\sigma_h^2 + \sigma_v^2$ as stated above and the following first p time lags $(\tau_1, \ldots \tau_p > 0)$ to obtain p estimates of f_c; $\hat{f}_c$ being the average value of these estimates. Similarly, we take the p largest time lags to estimate f_d. To estimate the noise variance, we form $\hat{\mathbf{R}}_x$ from the first $p + 1$ channel correlation estimates, $\hat{r}_x(0), \hat{r}_x(T_s), \ldots, \hat{r}_x(pT_s)$, by using the fact that it is WSS (implying that $\mathbf{R}_x$ has a Toeplitz structure). Knowing that $\mathbf{R}_h$ is approximately of rank 2 (the two-ray approximate model), we average the smallest $L < (p-1)$ (in our case $L = 10$) eigenvalues of $\hat{\mathbf{R}}_x$. This shows that the proposed procedure has a very low complexity. Indeed, the overall complexity is dominated by the eigenvalue decomposition with a complexity order of $O((p+1)^3)$ operations.

Since the channel's PSD is symmetric, $\hat{f}_c$ can be obtained without any approximation. In contrast, the simplified estimator of the Doppler spread factor in (22) is obtained thanks to the approximate form in (12) and (13) which slightly biases the estimator. To compensate this bias, we found through extensive simulations that by multiplying $\hat{\sigma}_f$ by a correction factor $\alpha = 1.14$, we can slightly improve our results. The new Doppler spread estimator is then given by

$$\hat{\hat{\sigma}}_f = \alpha \hat{\sigma}_f. \tag{25}$$

To sum up, we have shown in this contribution that the Doppler spread and CFO can be estimated at a low computational cost and with good accuracy when the channel's PSD is symmetric. This is actually an important gain as compared to many other methods where full knowledge of the analytical expression of the channel's PSD is required as in [2], [6], [7], and many other references. However, this assumption makes the proposed method applicable only in environments where the scattering is isotropic (i.e., all angles-of-arrival of the source are equiprobable). This is still the case for many methods in the literature [2], [3], [7], [8]. In anisotropic environments, the channel's PSD becomes asymmetric due to the directivity of the AOA of the scatterers [5], [6]. By observing the proof that led to the two-ray approximation in the Appendix [specifically, the transition from (26) to (27)], it is obvious to see that when the channel's PSD becomes asymmetric, the odd-order frequency moment terms may become significant, thereby breaking our two-ray approximation and deteriorating the performance of the proposed estimators.

V. Simulation Results

To illustrate the efficacy of the proposed method, we implement the data model in (1) using Jakes' model [1] which is commonly assumed in the literature. We run our simulations over T data samples and average the obtained results over $\mathrm{MC} = 10^3$ Monte Carlo runs for all the investigated scenarios.

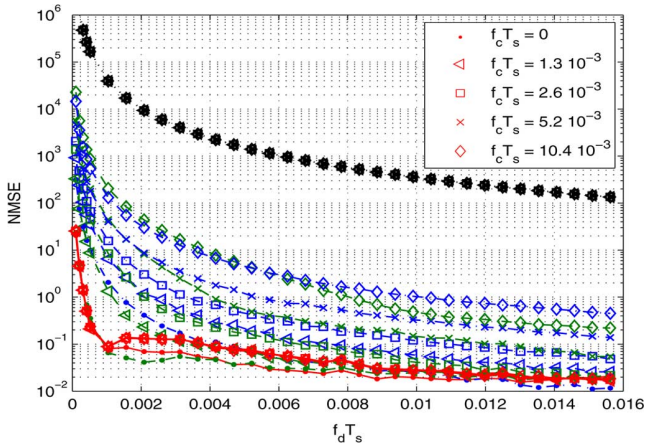

Fig. 2. NMSE(f_d) versus f_dT_s, SNR $= 0$ dB, $T = 1024$, and $f_cT_s = 0, 1.3\ 10^{-3}, 2.6\ 10^{-3}, 5.2\ 10^{-3}$, and $10.4\ 10^{-3}$, for the proposed estimator (solid/red), HAC (dashed/green), ML (semi-dashed/blue), and the method of Holtzman and Sampath (dotted/black).

The performance index that we use is the normalized mean squared error (NMSE) between the estimated and actual parameter of interest (σ_ω). We compare the proposed approach to the so-called "hybrid method for Doppler spread estimation" (denoted as HAC herein) proposed in [7] which is a combination of the methods proposed in [6] and [12], the ML-based method proposed in [2], and the Holtzman and Sampath's method which uses the autocovariances of the powers of the received signal envelope [17].

In Fig. 2, we present the variations of the NMSE over the estimation of f_d with respect to f_dT_s in the cases $f_cT_s = 0, 1.3\ 10^{-3}, 2.6\ 10^{-3}, 5.2\ 10^{-3}$, and $10.4\ 10^{-3}$ (recall that T_s is the sampling rate). It is important to note that these values are below the threshold of residual CFO tolerated by some standards such as 3 GPP after CFO recovery [8]. f_dT_s is varied between $1.04\ 10^{-4}$ and $1.56\ 10^{-2}$ at an SNR $= 0$ dB and a number of samples $T = 1024$. The ML approach provides poor estimates since it is based on the similarity between the hypothetical spectrum at $f_cT_s = 0$ and the actual one. The presence of a frequency shift due to the CFO deteriorates its performance. Similarly the performance of the HAC is affected by the CFO but is still better than ML for moderate CFO values. The Holtzman and Sampath's method is not affected by the CFO since it is based on the powers of the received signal envelope. However, it performs quite poorly due to the considered range of f_dT_s and the high level of noise. The proposed estimator is, in contrast, robust to the CFO and provides highly accurate results at very low Doppler spread values (even at around $f_dT_s = 10^{-3}$) typically encountered in vehicular high data-rate communications. The HAC method is able to nearly match the performance of our estimator only in the ideal case of no CFO.

Next, we choose $f_dT_s = 1.04\ 10^{-3}$ and $f_cT_s = 0, 1.3\ 10^{-3}$, $2.6\ 10^{-3}, 5.2\ 10^{-3}$, and $10.4\ 10^{-3}$ and assess the effect of the SNR variations on the four approaches in Fig. 3. The number of samples was chosen as $T = 1024$. The proposed estimator is able to achieve good estimates of σ_ω at very low SNR values (starting from 0 dB) while the ML and HAC clearly fail in the presence of a CFO. Two important factors account for the high bias observed with the latter two techniques even with high SNR: low f_dT_s and existence of the CFO. Both factors are commonly encountered in high data-rate transmission systems with the inevitable asynchrony between the communicating ends even after RF-domain down-conversion CFO recovery. Again, the Holtzman

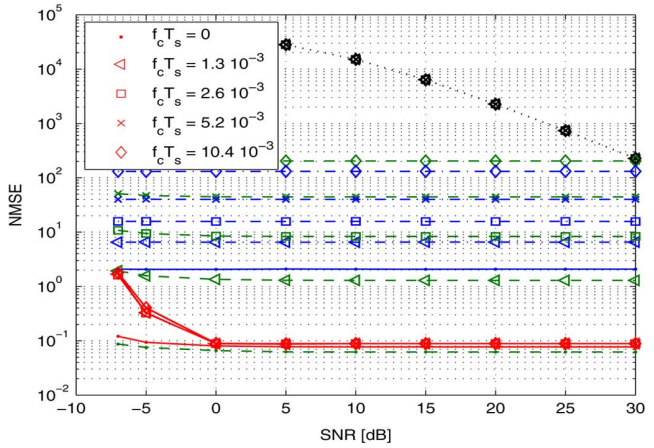

Fig. 3. NMSE($f_{\rm d}$) versus SNR, $f_{\rm d}T_{\rm s} = 1.04\ 10^{-3}$, $T = 1024$, and $f_{\rm c}T_{\rm s} = 0, 1.3\ 10^{-3}, 2.6\ 10^{-3}, 5.2\ 10^{-3}$, and $10.4\ 10^{-3}$ for the proposed estimator (solid/red), HAC (dashed/green), ML (semi-dashed/blue), and the method of Holtzman and Sampath (dotted/black).

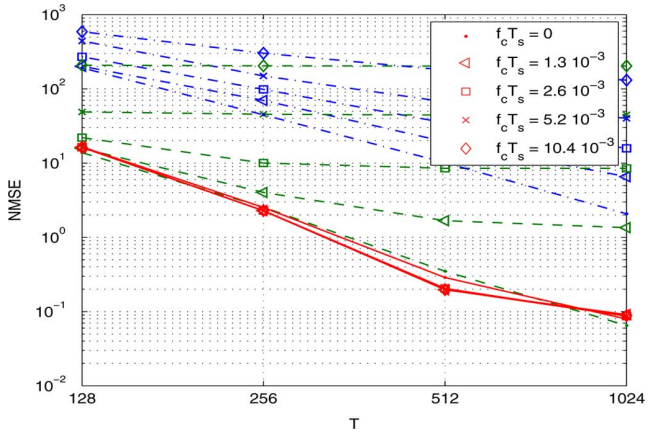

Fig. 4. NMSE($f_{\rm d}$) versus T at $f_{\rm d}T_{\rm s} = 10^{-3}$, SNR $= 0$ dB, and $f_{\rm c}T_{\rm s} = 0, 1.3\ 10^{-3}, 2.6\ 10^{-3}, 5.2\ 10^{-3}$, and $10.4\ 10^{-3}$ for the proposed estimator (solid/red), HAC (dashed/green), and ML (semi-dashed/blue).

and Sampath's method exhibits the same performance for all the CFO values since it is based on the covariance of the powers of the signals. Unfortunately, it fails to achieve acceptable accuracy even at very high SNR because of the low value of $f_{\rm d}T_{\rm s}$. For this reason, the latter method will be discarded from the following comparison.

We also investigate the effect of the number of data snapshots on the performance of the three approaches. As expected, using fewer samples increases the second-order statistics estimation errors, thereby deteriorating the performance of the three methods. This fact is illustrated in Fig. 4 where we chose SNR $= 0$ dB, $f_{\rm d}T_{\rm s} = 1.04\ 10^{-3}$, and varied the number of data snapshots. A remarkable robustness of the proposed estimator to the CFO as compared to the other methods is achieved especially when the CFO increases.

In real-world systems, the CFO is unpredictable and can be modeled as a random variable [16]. The proposed Doppler spread estimator has the advantage of automatically compensating this artifact. The simulation results provided above illustrate the efficiency of our method for a wide range of values that can be taken by the CFO. It is also worth noting that the estimation of the Doppler spread is more challenging at low $f_{\rm d}T_{\rm s}$ values. In high data-rate transmission systems (e.g., future-generation wireless networks), these values are more likely to be encountered even at high mobile speed (or maximum Doppler frequency) since $T_{\rm s}$ can be very small. It is quite remarkable that the proposed approach provides accurate estimates at a very low range of $f_{\rm d}T_{\rm s}$. This fact makes it a good candidate for systems that require robust Doppler estimates not only for mobile velocity estimation, but also for optimal adaptive processing in vehicular communications where the optimal adaptation step-size is directly related to the Doppler spread estimate [13].

The proposed method also allows for the estimation of the CFO as it has been clearly shown in (23). To assess the performance of this built-in estimator, we compare it to the method proposed in [8] which is based on the adaptive estimation of the channel using the stochastic least mean square algorithm and a linear regression over the phase of the channel estimate, and the unweighted linear regression proposed in [14]. The parameters required by the method of [8] were set to obtain the best performance in the investigated scenario and the same range of time delays required by our approach was used for the method of [14] although no clear rule was mentioned therein about this choice. We use the same setup (as the one used for the previous numerical examples) and analyze the effect of the maximum Doppler frequency, $f_{\rm d}T_{\rm s}$, the number of samples, and the input SNR on the variations of the NMSE over the CFO. The results are depicted in Fig. 5. Note that the estimate of the CFO in [8] is derived from the estimate of the channel which is biased by the presence of the additive noise. Hence, the resulting CFO estimator is affected. This fact becomes more obvious when operating with low number of samples and/or low SNR. The unweighted linear regression method exhibits comparable performance to the proposed one especially for low $f_{\rm d}T_{\rm s}$ values. For larger values, our method seems to offer better accuracy. The estimation of low CFO values is more difficult than large ones. The residual CFO is, indeed, inevitable in communication systems and taking it into account when assessing Doppler spread estimation techniques is essential.

VI. Conclusion

In this correspondence, we proposed a new Doppler spread estimation method. This approach is robust to the residual carrier frequency offset which is inherent to the physical limitations of the oscillators at the communicating ends in a wireless link to properly operate at a given frequency. We first showed that the Doppler spread estimation in environments with isotropic scattering is very similar to addressing the issue of AS and nominal AOA estimation in the case of locally and incoherently distributed sources. Then, we took advantage of the typical small channel frequency fluctuations (relative to the sampling rate) around the CFO due to the Doppler effect to develop a two-ray spectrum approximation and deduce a simplified Doppler spread estimator which automatically compensates the CFO. A robust CFO estimator was also developed as a byproduct of this contribution. Simulation results were finally provided to corroborate the effectiveness of our technique, especially in the most challenging conditions for parameter estimation: low SNR, small Doppler spread, high data-rate transmissions, and large residual CFO.

Appendix
Proof of the Two-Ray Approximate Model

A similar proof can be found in [11] with application to the AS and nominal AOA estimation in the case of spatially distributed sources. We first define $\mathbf{a} = \mathbf{a}(\omega_{\rm c})$, $\mathbf{d} = \partial\mathbf{a}(\omega)/\partial(\omega T_{\rm s})|_{\omega=\omega_{\rm c}}$, $\mathbf{r} = \partial^2\mathbf{a}(\omega)/\partial(\omega T_{\rm s})^2|_{\omega=\omega_{\rm c}}$. By virtue of Assumption 2, we have

$$\omega_{\rm d}T_{\rm s} = 2\pi f_{\rm d}T_{\rm s} \ll 1.$$

For $\omega \in [-\omega_{\rm d}, \omega_{\rm d}]$, we also have $|\omega|T_{\rm s} = 2\pi|f|T_{\rm s} \ll 1$. Therefore, we use the following second-order Taylor series

$$\mathbf{a}(\omega + \omega_{\rm c}) \approx \mathbf{a} + (\omega T_{\rm s})\mathbf{d} + \frac{(\omega T_{\rm s})^2}{2}\mathbf{r}.$$

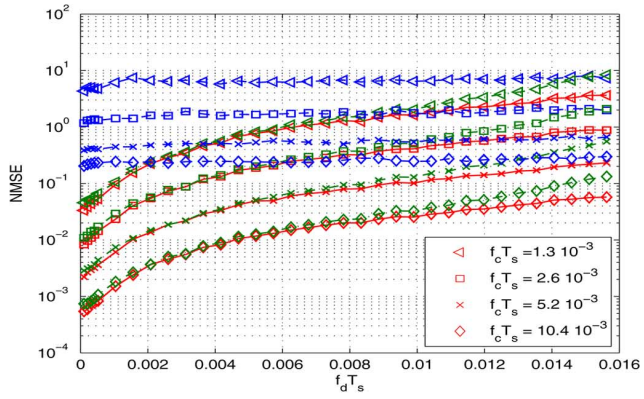

(a)

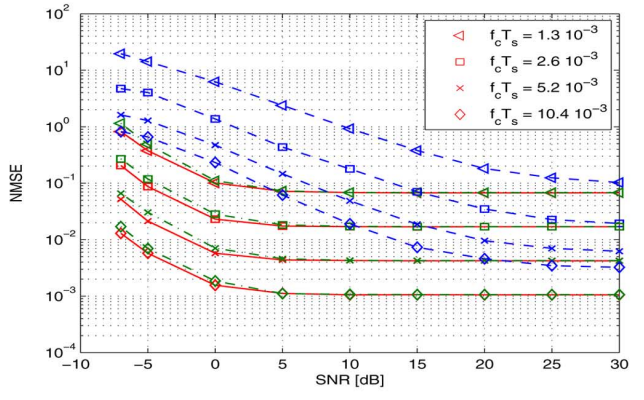

(b)

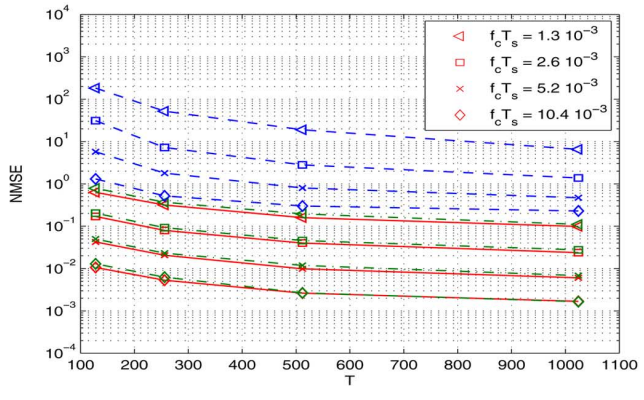

(c)

Fig. 5. Performance of the CFO estimator: (a) NMSE(f_c) versus f_dT_s; $T = 1024$; SNR $= 0$ dB, (b) NMSE(f_c) versus SNR [dB]; $T = 1024$; $f_dT_s = 1.04\ 10^{-3}$, and (c) NMSE(f_c) versus T; SNR $= 0$ dB and $f_dT_s = 1.04\ 10^{-3}$. Proposed estimator (solid/red), method of [8] (dashed/blue), and method of [14] (semi-dashed/green).

Using the above approximation and (10), we obtain

$$\mathbf{R}_h \approx \sigma_h^2 \int_{-\omega_d}^{\omega_d} \tilde{S}(\omega) \left[\mathbf{a}\mathbf{a}^H + (\omega T_s)(\mathbf{d}\mathbf{a}^H + \mathbf{a}\mathbf{d}^H) + \frac{(\omega T_s)^2}{2}(2\mathbf{d}\mathbf{d}^H + \mathbf{r}\mathbf{a}^H + \mathbf{a}\mathbf{r}^H) + \frac{(\omega T_s)^3}{2}(2\mathbf{d}\mathbf{r}^H + \mathbf{r}\mathbf{d}^H + \mathbf{a}\mathbf{r}^H) + \frac{(\omega T_s)^4}{4}\mathbf{r}\mathbf{r}^H \right] d\omega. \quad (26)$$

Using Assumption 1, we get rid of the terms $\propto \omega$ and $\propto \omega^3$ in the above integral. We also neglect the term $\propto (\omega T_s)^4$ thanks to Assumption 2. Then, (26) simplifies to

$$\mathbf{R}_h \approx \sigma_h^2 \left[\mathbf{a}\mathbf{a}^H + \frac{(\sigma_\omega T_s)^2}{2}(2\mathbf{d}\mathbf{d}^H + \mathbf{r}\mathbf{a}^H + \mathbf{a}\mathbf{r}^H) \right]. \quad (27)$$

Again, by virtue of Assumption 2, we can add an extra-term $((\sigma_\omega T_s)^4/4)\mathbf{r}\mathbf{r}^H$ to the right-hand side of (27). Then, we obtain

$$\mathbf{R}_h \approx \frac{\sigma_h^2}{2} \left\{ \left[\mathbf{a} + (\sigma_\omega T_s)\mathbf{d} + \frac{(\sigma_\omega T_s)^2}{2}\mathbf{r} \right] \times \left[\mathbf{a} + (\sigma_\omega T_s)\mathbf{d} + \frac{(\sigma_\omega T_s)^2}{2}\mathbf{r} \right]^H + \left[\mathbf{a} - (\sigma_\omega T_s)\mathbf{d} + \frac{(\sigma_\omega T_s)^2}{2}\mathbf{r} \right] \times \left[\mathbf{a} - (\sigma_\omega T_s)\mathbf{d} + \frac{(\sigma_\omega T_s)^2}{2}\mathbf{r} \right]^H \right\}. \quad (28)$$

Now, we can still make the following approximations thanks to Assumption 2 ($\sigma_\omega T_s \ll 1$):

$$\mathbf{a}(\omega_c + \sigma_\omega) \approx \mathbf{a} + (\sigma_\omega T_s)\mathbf{d} + \frac{(\sigma_\omega T_s)^2}{2}\mathbf{r} \quad (29)$$

$$\mathbf{a}(\omega_c - \sigma_\omega) \approx \mathbf{a} - (\sigma_\omega T_s)\mathbf{d} + \frac{(\sigma_\omega T_s)^2}{2}\mathbf{r}. \quad (30)$$

By plugging (29) and (30) into (28), we obtain the two-ray approximation in (12) and (13). ■

REFERENCES

[1] W. C. Jakes, *Microwave Mobile Communications*. New York: IEEE/Wiley, 1974.

[2] H. Hansen, S. Affes, and P. Mermelstein, "A Rayleigh Doppler frequency estimator derived from maximum likelihood theory," in *Proc. IEEE SPAWC*, 1999, pp. 382–386.

[3] G. Park, D. Hong, and C. Kang, "Level crossing rate estimation with Doppler adaptive noise suppression technique in frequency domain," in *Proc. IEEE Vehicular Technology Conf. (VTC)—Fall*, 2003, pp. 1192–1195.

[4] M. D. Ausint and G. L. Stuber, "Velocity adaptive handoff algorithms for microcellular systems," *IEEE Trans. Veh. Technol.*, vol. 43, no. 3, pp. 549–561, Aug. 1994.

[5] K. Baddour and N. C. Beaulieu, "Robust Doppler spread estimation in nonisotropic fading channels," *IEEE Trans. Wireless Commun.*, vol. 4, no. 6, pp. 2677–2682, Nov. 2005.

[6] C. Tepedelenlioglu and G. B. Giannakis, "On velocity estimation and correlation properties of narrowband mobile communication channels," *IEEE Trans. Veh. Technol.*, vol. 50, no. 4, pp. 1039–1052, Jul. 2001.

[7] O. Mauritz, "A hybrid method for Doppler spread estimation," in *Proc. IEEE Vehicular Technology Conf. (VTC)—Spring*, 2004, pp. 962–965.

[8] S. Affes, J. Zhang, and P. Mermelstein, "Carrier frequency offset recovery for CDMA array-receivers in selective Rayleigh-fading channels," in *Proc. IEEE Vehicular Technology Conf. (VTC)—Spring*, 2002, pp. 180–184.

[9] R. H. Clarke and W. L. Khoo, "3-D mobile radio channel statistics," *IEEE Trans. Veh. Technol.*, vol. 46, no. 3, pp. 798–799, Aug. 1997.

[10] M. Souden, S. Affes, and J. Benesty, "A two-stage approach to estimate the angles of arrival and the angular spreads of locally scattered sources," *IEEE Trans. Signal Process.*, vol. 56, no. 5, pp. 1968–1983, May 2008.

[11] M. Bengtsson and B. Ottersten, "Low-complexity estimators for distributed sources," *IEEE Trans. Signal Process.*, vol. 48, no. 8, pp. 2185–2194, Aug. 2000.

[12] D. Sandberg, "Method and Apparatus for Estimating Doppler Spread," U.S. Patent 6922452, application no. 09/812956, Mar. 27, 2001, prior publication data: US 2002/0172307 A1 Nov. 21, 2002, issued on July 26, 2005.

[13] S. Affes and P. Mermelstein, , J. Benesty and A. H. Huang, Eds., "Adaptive space-time processing for wireless CDMA," in *Adaptive Signal Processing: Application to Real-World Problems*. Berlin, Germany: Springer, Feb. 2003, ch. 10, pp. 283–321.

[14] O. Besson and P. Stoica, "On frequency offset estimation for flat fading channels," *IEEE Commun. Lett.*, vol. 5, no. 10, pp. 402–404, Oct. 2001.

[15] M. Souden, S. Affes, and J. Benesty, "A two-ray spectrum-approximation approach to Doppler spread estimation with robustness to the carrier frequency offset," in *Proc. IEEE SPAWC*, 2008, pp. 31–35.

[16] B. Smida, S. Affes, L. Jun, and P. Mermelstein, "A spectrum-efficient multicarrier CDMA array-receiver with diversity-based enhanced time and frequency synchronization," *IEEE Trans. Wireless Commun.*, vol. 6, no. 6, pp. 2315–2327, Jun. 2007.

[17] J. Holtzman and A. Sampath, "Adaptive averaging methodology for handoffs in cellular systems," *IEEE Trans. Veh. Technol.*, vol. 44, no. 1, pp. 5966–, Feb. 1995.